CHAPTER 6

THE MODIFIED AMSLER WEAR MACHINE. DESCRIPTION, TEST PROGRAMME and VIBRATION ANALYSIS

6.1 Introduction

The most well known machine for assessing dry rolling-sliding wear behaviour is the Amsler. It was designed in the 1920's, primarily for the examination of rail steel wear[Amsler, 1922]. It consists of simple mechanical components with a single 3 phase, two speed, electric motor. Its universal appeal has not diminished and the design has not been fundamentally changed to the present day. Many other rolling-sliding wear machines are of a similar design, though modified, eg, Japan (Nishihara machine)[Ichinose et al, 1978, Masumoto et al, 1978] and the former USSR[Vekser et al, 1970]. Such machines enable two discs of test material to be rolled under pressure, with a degree of sliding. The Amsler disc drives have a geared $\approx 10\%$ speed differential (the Nishihara machine has a few additional gear selections), other degrees of slip / creepage, must be obtained by varying disc diameters. A normal load is applied via one of two calibrated springs. The machine can also be used for pin on ring, pure sliding tests (i.e. one disc rotating against a static pin or disc).

Part of the wear test programme described in this thesis was carried out on a modified Amsler machine, kindly loaned by the British Rail Technical Centre, Derby, UK. The performance of, and results from, this machine were used as a basis for the construction of an in-house wear machine built on a standard lathe base, the **LE**icester **RO**lling and **S**liding wear machine (**LEROS**), and for a comparative evaluation of tests carried out on LEROS.

Under certain conditions, the wear surfaces of discs tested on both wear machines developed periodic plastic deformation patterns on their wear tracks. In the present work, these these track wide undulations have been termed corrugations (wavelengths $<$ 1mm) and facets (wavelengths $>>$ 1mm). Additionally, with severe wear, surface ripples formed with a similar degree of regularity to some

facets. Regular patterns of deformation are common phenomena for surfaces in rolling and rolling-sliding contact. Similar axial deformations (wavelengths > 20mm) form on railway rails, these are termed "corrugations", as described in the previous chapter. The material and operational factors which result in such deformations are not yet fully understood, despite over one hundred years of study. They are still subject of intense academic debate[Knothe and Gasch, 1983]. With respect to this work, their effect on the pattern of wear test results was examined and an investigation was carried out into whether such deformations could be linked to machine vibrations. This investigation, with respect to the modified Amsler machine, is described in Section 6.5.

6.2 The modified Amsler wear machine - a description.

The machine is shown in Figure 6.1 and a schematic description of its components, together with gearing contact details, in Figure 6.2. For comparison, a schematic representation of a standard Amsler machine is shown in Figure 6.3. The loading system of the machine was further modified at Leicester University for some of the wear tests where machine vibrations were monitored; this is schematically described in Figure 6.4. British Rail had initially modified the machine by adding a split pivoting base with a flexible drive link to the top disc gearing and bearing assembly. This enabled tests with angular displacement of disc axes (yaw) to be carried out. This yaw facility was ***not*** used during any of the tests described here, but this modification had two effects: (a) The standard Amsler disc size of 35mm diameter was not suitable; 42mm discs were used, and (b), machine vibrations were affected by the flexible drive (this is discussed in Section 6.5).

The mechanical torque dynamometer had been modified by British Rail so that the mechanical pen action was replaced by a linear velocity displacement transducer (LVDT). Early in the test programme (after Test 6) this facility was further modified at Leicester. The weights, associated mechanical graph logging facility and the LVDT were removed from the pivoting dynamometer arm. A rigid plate was fixed to the underside of the machine base. A linear load transducer was connected to the pivoting arm and, except at zero load, this pressed against the rigid plate, thus

making the arm essentially rigid. Torque was calculated (and plotted) from the transducer millivolt output. A more sensitive read-out was achieved in this manner. This modification is shown in Figure 6.5. The load cell millivolt output was also connected, via an adjustable trip amplifier, to the emergency stop circuit. This replaced the mechanical overload trip, which had been activated by maximum pivoting of the dynamometer arm. The stop circuit was also triggered by opening the safety cage or by leaving a locking bar in the gear assembly.

An environment chamber was fitted to the machine. Its metal base was attached to the bottom bearing housing. Once a top disc had been fitted, and the top bearing housing swung down to make disc contact (Figures 6.6 and 6.7), the perspex top of the environment chamber was located. Within the chamber, blasts of dry compressed air both cooled the discs and kept the 5mm wide wear tracks free of loose debris, thus simulating moving wheel on rail contact. The blasts were from two elliptical nozzles (inside dimensions - 5mm major horizontal axis, 2mm minor vertical axis) which were situated between 3 to 5mm from each disc wear track, both slightly angled toward the roll exit gap. An initial compressed air supply of 6.33 kg/cm^2 (90 psi) dropped to a steady 1.0 kg/cm^2 (14.2 psi) once the air blast was operational.

Debris laden air was drawn from the environment chamber via a 6.6mm diameter vacuum tube within its base. This was fitted to a household vacuum cleaner, via a filter assembly. An offshoot from this air exit tube (out of the air flow) contained a probe which measured exit air temperature and humidity (Figure 6.1). Within the environment chamber the vacuum output slightly exceeded the air input, thus ensuring rapid debris clearance.

The exit air passed through a filter box. This has two, 25mm diameter, coarse filter grids. Both contain 0.4mm square holes. One of these could be used to support a fine 25mm diameter, cellulose nitrate, membrane filter. The membrane filter used had a pore size of 1μm. Insertion of the membrane filter seriously affected the exit air flow and thus disrupted (the steady state portion of) the test. For this reason, fine debris was only collected at the termination of a few, selected tests, once steady state

wear behaviour had been established. The 0.4mm coarse filter was used during all tests. For most tests, it was checked at each weighing stage and emptied if required. During some particularly severe tests it was emptied more frequently. Exit air blockage was reflected in a deviation from the steady state torque output.

6.3 Limitations of the Amsler wear machine.

Control of creepage.

The machine has a single, fixed, geared differential between the top and bottom shaft rotational speeds of 1.104, with the top shaft slower. This gives an initial creepage, with discs of equal diameter, of 9.89%. For any other value, the discs have to be machined to different diameters, therefore each pair of discs is tied to a set test condition and a standardised stock of discs is not possible. Once a pair of discs have begun to wear, it is not possible to trim creepage back to the initial set value. If wear of one of the discs is particularly heavier than the other, the creepage deviation can be considerable. Just the factor of having a geometric difference between disc pairs, such as a different diameters, has in itself been shown to affect wear rates[Krause and Lehna (1987)].

Application of normal load.

A load is normally applied via one of two springs; the load value being read from a coarsely engraved rule. The maximum load that can be applied is 2335N (238kg), therefore with standard cylindrical discs of around 39 to 42mm in diameter, and 5mm track widths, the highest value of maximum contact stress that can be applied is limited to around 1300 MPa. (Further reductions in track width would increase the significance of plastic collapse at the disc track edges.) Where a constant value of contact stress is required, whilst disc diameters vary, accurate trimming of the load is difficult to achieve.

Disc location.

Discs are secured on to the respective bearing shafts by tightening a nut along the threaded end of the shaft. To avoid subsequent mechanical damage to the disc shoulders, and any associated weight loss, two 0.17mm thick paper washers are used

per disc. Neither disc drive shaft is keyed, thus there is a consequent risk of disc slippage around the shaft and there is no circumferential datum position of either disc with respect to their locations on the shafts. For all Amsler tests described in this text, the shaft nuts were tightened against the discs at a torque of 54 Nm; no slippage was observed. Paper washers had to be replaced at most weighing intervals.

Disc alignment.

Precise transverse alignment of the two 5mm wide disc wear tracks is dependent upon the dimensional accuracy of each disc inner shoulder and the thickness of the paper washers used. There is no facility on the Amsler machine for trimming the alignment. Discs were machined to the tolerances shown in Figure 6.8.

Torque output.

The torque monitoring components appeared to be subject to considerable high frequency accelerations, such that the output has to be filtered in order to achieve a meaningful trace on a chart recorder.

6.4 The test programme on the modified Amsler wear machine.

After an initial couple of tests to assess machine functioning, where rail steels were not used, a test programme was established (Table 6.1). The first six tests of the programme were used to assess the significance of individual test variables, after which a more standardised procedure was adopted. Pearlitic BS11 rail and Type 'D' tyre discs were used for Tests 3 to 11, so that a test procedure relating to test conditions could be established and the results compared with other Amsler results on these materials[Bolton et al. 1982; Bolton & Clayton, 1984]. Test conditions and variables are discussed below, with the exception of periodic, wear surface plastic deformations. These are discussed in Section 6.5.

Variables.

Grainflow within a disc.

Where a disc was cut longitudinally along from a railhead, the longer axis of elongated grains would be parallel to the wear track at two circumferential points

only and normal to the wear track at right angles to those points, i.e. an inhomogenous surface. Therefore in this work, except for that experiment, all discs were machined from a cross-section of (hot rolled) railhead which would result in elongated grains across the wear track at all circumferential positions, i.e. homogenous wear track surfaces. Bainite discs were similarly machined from transverse slices of hot rolled bar and wheel discs from "cheese" sections cut around forged and rolled railway wheel rims/tyre. Changing the grainflow direction of the driven R52 rail disc was found to have an small effect on wear rates, mainly of the counterface disc (Figure 6.9). These grainflow effects are of significance for commercial pearlitic rail steels which normally contain a sizeable distribution of elongated manganese sulphide inclusions. These inclusions are thought pertinent to the wear process; this is discussed in Chapter 10.

Weight loss measuring intervals.

Early tests were used to "feel" a way toward a standardised experimental procedure. The effect on wear rates of changing weight loss measuring intervals, in combination with other procedural changes*, can be seen in Figure 6.10. [* It was after Test 6 that the standard Amsler weight balanced, swinging dynamometer was replaced by a rigid arm, plus load cell, for the measurement of torque. This made the bottom disc drive more "steady state" and less "dynamic". In addition, the air nozzles were slightly re-aligned as mentioned in Section 6.2 and air pressure increased from 0.7 to 1.0 kg/cm^2 (10 to 14 psi).].

These early tests showed that there was an extensive running-in period. This is clearly shown by the Test 7 wear curve in Figure 6.10. To map this period accurately, a standardised procedure was adopted with weighing intervals at 2, 4, 7, 10, 15, 20, 25 and 30 thousand bottom discs revolutions, followed by measurements at every 10,000 revolutions up to 100,000 total revolutions and, after that (i.e. for longer "mild wear" tests), every 20,000 revolutions. With frequent measuring intervals, long interruptions in a test run appeared to affect a wear curve, however such an effect was minimal once the established testing procedure was used. Most tests were completed within one or two days. With short life, severe wear tests,

weighing intervals were more frequent and steady state was rapidly established. The comparative review of wear results in Chapter 8 is based on tests which had established testing procedures, i.e. from Test 7 onward.

Disc dimensions.

To vary creepage or slip away from 10% on an Amsler machine, disc diameters must be varied. In this programme of tests, top (driven / braking) rail disc diameters were standardised at 42mm. Bottom (driving) discs, manufactured from the standard reference material W64 (Type 'D' tyre), had variable diameters. The mechanical properties of the two pearlitic materials, R52 and W64, are broadly similar (Table 2.3, Figure 2.21a), as are their microstructures. During the wear test programme, it was observed that where the bottom disc diameter was smaller than that of the top disc, the bottom disc wear rate was higher and where the bottom disc had a larger diameter, its wear rate was comparatively lower (see Chapter 8 - Wear Test Results). A "disc diameter effect" has been observed by other workers[Krause and Lehna, 1987].

Test environment humidity and temperature and disc temperatures.

A volume of dry, compressed air was blasted into the environment chamber (at the disc tracks) and a slightly greater volume of air was vacuumed out. Therefore some laboratory air was drawn into the chamber, thus producing small fluctuations in humidity. Over the complete test programme, mid-test humidity varied between 15% and 50% RH; for most tests it was between 25% and 40% RH. No correlation was found between these variations in humidity and respective coefficients of traction (Figure 6.11).

The environment chamber air-flow would absorb nearly all of the frictional heat generated by the discs. Again, there were slight fluctuations dependent upon test conditions; temperatures would rise by no more than 5°C during a test run of 10000 revolutions under severe conditions. The humidity and temperature of air leaving the chamber were constantly monitored.

Disc surface temperatures were monitored by a contact thermometer during weighing intervals, immediately the discs had come to rest. For most tests, temperatures were less than 10°C above room temperatures. For the most severe tests, disc bulk temperatures never exceeded 20°C above room temperature. Some results are shown in Table 6.2. The slight differences in disc bulk temperatures between the material combinations were not reflected by the differences in wear rates.

6.5 Vibration analyses of the modified Amsler wear machine.

Within the Engineering Department of Leicester University a final year undergraduate project, carried out by J.R. Brightling and overseen by the author and J.H. Beynon, examined the effect (on wear rates, test disc surface deformation and machine vibrations) of substituting the conventional Amsler spring loading system with a rigid loading system. The paper appended to this thesis [Garnham, Brightling and Beynon, 1988] combines Brightling's results with the author's observations on Amsler disc surface plastic deformations and respective test conditions resulting from the test programme described in Section 6.4. A further vibration analysis, at both machine speeds, has been carried out by the author, in tandem with an analysis of the LEROS machine (separately reported in Chapter 7). Vibrations at the slower Amsler machine speed were not examined in Brightling's study. This further analysis is discussed below. The full disc plastic deformation results for the Amsler tests in the present work are shown in Table 6.3 and periodic undulation patterns are mapped against test conditions, for all the materials, in Table 6.4.

Experimental procedure

Vibration measurement.

A Bruel and Kjaer Type A4328 accelerometer was used (with a magnetic base) coupled to an Ono Sokki CF-910 Fast Fourier Transform Frequency Analyser. The accelerometer output was processed through a Bruel and Kjaer Vibration Pick-up Preamplifier Type 2625, whose output could be set to register accelerations, or their first integral with respect to time, velocities; or their double intergral, displacement. This integration process can also be viewed as a high pass filter to the vibration spectrum. For most tests in this work, frequency spectra for accelerations and

velocities have been examined. The integrated millivolt outputs for velocity frequencies were reduced compared to the direct acceleration frequency outputs. High acceleration frequencies had their amplitudes "filtered down" in the velocity frequency spectra.

The accelerometer location on the bottom disc bearing housing was the same as that used by Brightling, the flat base flange (Figure 6.7). The author chose an alternative site to Brightling for locating the accelerometer on the top bearing housing, a flat flange area where there was a more secure base for the magnetic probe. Both locations are shown in Figure 6.7.

Test procedure.

The natural resonances of the modified Amsler machine were examined; the motor was switched off and test discs were in static contact. The cylindrical discs were loaded to give 500 MPa maximum contact stress. During the wear test programme it was at this contact stress, combined with a creepage of 10%, that the clearest periodic surface plastic deformations were formed with the machine running at the higher speed setting (386 bottom disc rpm). The machine was excited by resonating the frame near the area of disc contact with a hammer. A frequency spectrum was obtained, averaged from the spectra of 32 hammer blows. Both a steel hammer and a soft hammer were used and the results compared. (Brightling had used a steel hammer for his tests.) With hammer contact, the strength of signals across the averaged frequency spectra must be dependent upon the arbitary force used for each blow, however it is valid to make a comparison of signal strengths at specific frequencies across a spectra.

Machine resonances were measured with the machine free running at the two machine speeds (193 and 386 bottom disc rpm). As there were no discs fitted, the top bearing housing was pivoted down against the lower frame (in the test position) and loaded, at the same setting as above, against a 10mm thick rubber. In all assessments with the machine running, the average of 256 spectra was taken by the analyser, for each frequency range setting.

A worn pair of Brightling's discs (R52 top disc and W64 bottom disc) were refitted and re-run under the same test conditions - 500 MPa maximum contact stress with spring loading, 10% creepage and 386 bottom disc rpm. Vibration spectra were compared. For the previous test details, refer to the sixth column of Table 2 in the appended reference[Appendix I - Garnham, Brightling and Beynon, 1988]. For examining machine resonances at the lower machine speed (193 bottom disc rpm), a worn R52/W64 pair from one of the author's tests were re-fitted to the machine and re-run at 500 MPa maximum contact stress and 10% creepage. Previous test details are shown in the seventh column of Table 2 in the appended reference.

Summary of vibration analysis.

A summation of results is given in Tables 6.5, 6.6 and 6.7. Sets of readings were taken over several "X-axis" frequency ranges (0 → 10, 5, 2 and 1 kHz). As the range was decreased, it was often the case that signals at a peak frequency area were spread along more of a "digitised space" on the signal display X-axis, with a consequent drop in the signal amplitude. What appeared to be a single peak at a high range was revealed as a close-knit group of peaks at a low range. The general pattern of any part of a spectra remained the same. Most of the "comparative" signal strength values quoted in Tables 6.5, 6.6 and 6.7 have been taken from spectra over a specific frequency range (0 → 5 kHz). Occasionally signals strengths from the 0 → 10 kHz range have been included and/or a strength value covering a range of adjacent peaks.

The results have been reviewed with respect to the gear tooth impact frequencies and shaft speeds of the modified Amsler machine. These are shown, together with a schematic diagram of the machine, in Figure 6.2.

Natural resonances.

With both soft and hard hammers, at both bearing housing locations, the major natural resonance generated for both accelerations and velocities was around 500 Hz (Table 6.5). There were secondary resonances around 675 and 1025 Hz. When a steel hammer was used, there were extra significant accelerations around 5000 Hz,

but no significant velocities. High resonances around 1550 Hz produced with the steel hammer were greatly reduced when using the soft hammer. With either hammer, the author did not generate the acceleration peaks around 437.5 and 2000 Hz that Brightling recorded. Brightling had linked the 2000 Hz acceleration resonance to the generation of corrugations. Examples of spectra using both hammers are shown in Figure 6.12.

Machine free running.

For both accelerations and velocities, at the higher speed setting a frequency of 425 Hz was dominant and at the lower speed setting both 425 Hz and 210/212.5 Hz (Table 6.6). The frequency of tooth contact from the additional flexible shaft gears is 420 and 210 Hz at the two respective speeds (Figure 6.2). The higher of the two frequencies would probably have been amplified by the 500 Hz natural machine resonance described above. This may also have influenced the 625 Hz resonance registered at the bottom bearing housing location at both machine speeds. From the top bearing housing location, relatively weak signals of both acceleration and velocity at 50 Hz (high speed) and 62.5 Hz (low speed) were monitored. These may be of significance as they are near the frequency of the test disc facets which have been generated at both machine speeds. These high speed results matched those of Brightling.

Machine running under load with worn discs.

The work in the appended reference[Appendix I - Garnham, Brightling and Beynon, 1988] showed that where corrugations formed, if the machine speed was halved the corrugation wavelength remained the same, hence corrugation frequency was halved. However the frequency of the gross disc plastic deformations, termed "facets", remained constant when the machine speed was halved, hence their wavelength was halved. Facet severity was greatly reduced at the lower machine speed.

For the worn discs re-used again in this second series of tests, the facet and corrugation frequencies are given in Table 6.7, together with the respective principal frequencies of accelerations and velocities from the spectra generated by the worn

discs at the two machine speeds. There were two principal resonances; one at 62.5 Hz, presumably generated by disc facets and the second at 425 Hz (high speed) and 425/212.5 Hz (low speed), this was thought to be generated by the flexible drive gearing. It should be noted that discs tested on a standard (non-yawing) Amsler machine at the Railway Technical Centre (Derby, UK) also formed corrugations and facets[Appendix I - Garnham, Brightling and Beynon, 1988; Table 2, Column 23 (Suffix 'f')]. That machine had no flexible drive.

At high speed, no significant resonances were generated that matched the corrugation frequencies of 2121 Hz (top disc) and 2178 Hz (bottom disc), unlike Brightling's results[Appendix I]. Spectra from Brightling's results and the author's subsequent results are comparatively presented in Figures 6.13 and 6.14, respectively. At the slower machine speed there was a small resonance (acceleration only) of the top bearing housing (1112.5 Hz) near the disc corrugation frequencies (1193 Hz top disc, 1238 Hz bottom disc), but no bottom bearing housing resonance.

The resonance around 600/625 Hz, observed with the machine free running, was also present at both machine speeds during these loaded tests. This frequency would be reinforced by the tenth harmonic of the faceting frequency.

Discussion.

Where there is rolling or rolling-sliding contact between materials, under certain conditions, regular plastic deformations of the contacting surfaces may develop, eg., corrugations on rails. This phenomenon has been observed on numerous rolling and rolling-sliding tribology test machines. Over a hundred years of investigation has shown that there are no simple relationships linking mechanical and material considerations to the conditions under which such deformations form[Appendix I -Garnham, Brightling and Beynon, 1988].

The two limited vibration assessments of the modified Amsler machine, used for part of this series of wear tests, have shown that there are no strong natural resonances of the machine which correspond to any resonances, measured as accelerations and

velocities, generated by disc surface plastic deformations. The equipment amplification was not powerful enough to measure displacements; subsequent vibration work has found these significant[Pupaza and Beynon, 1994]. These results are discussed below. Amsler disc facets form slowly once a test has been underway for some time, but then to such an extent that a major resonance is generated. Brightling showed that changing to a more rigid form of disc loading had no effect on this phenomenon.

At the higher speed setting, the "yaw gearing" modification of this particular Amsler machine generated a strong resonance which was near the frequency of the dominant natural resonance of the static machine assembly. It was not determined whether this resonance had any influence on the formation of disc surface plastic deformations.

The formation of such deformations has an effect on wear behaviour, though generally not a major effect. This is described and discussed in Chapters 8 and 10.

Recently, further vibration studies have been carried out this modified Amsler machine[Pupaza and Beynon, 1994] after its disassembly and removal to another location. Most of vibration characteristics of the loaded and unloaded machine, described in this section, were confirmed. Similar low frequency facets were formed at the test condition of 5% creepage and 500 MPa maximum contact stress, but not the higher frequency corrugations. (During all Amsler wear tests for BS11 rail (R52) described in this work, high frequency corrugations formed under these conditions.) Again, there were good correlations between the degree of surface deformation, as measured by disc talyrond profilometry, and the facet vibration component, which Pupaza and Beynon found to have a typical initiation frequency around 58.2 Hz. As found in this work, the regular spacing of facets could degenerate with continued testing. Correlation between the predominant peaks of displacement spectra and the higher harmonics of rotational frequecy were detected. It was shown that vibration *displacements* were more suitable for monitoring rolling-sliding wear machine tests, than vibration accelerations. This author found that double integrating accelerations through the preamplifier to give displacements (i.e. high pass filtering; cf. second

paragraph of this section) resulted in too weak a response for meaningful measurement. Pupaza and Beynon overcame this by using separate eddy current displacement probes.

Pupaza and Beynon identified three distinct zones for accelerations;

(1 Hz - 1000 Hz). This covered the gear excitation frequencies, with a high level at 475 Hz due to the additional gearing (which these authors felt might have been faulty, hence the strong vibration) and/or the presence of a natural resonance.

(1500 - 3000 Hz). This range matches the frequencies of the fine wavelength corrugations that developed during tests described in this thesis, though these did not during Pupaza and Beynon's survey.

(4000 - 6000 Hz). This was found to cover the natural frequencies of the whole structure; 4950 Hz being dominant as it was possibly excited by the 11th harmonic of the (flexible) gear meshing frequency. Top rail disc facets were found to reach their maximum amplitude, before degeneration, at this frequency. This author found that this frequency was strong with the machine static (Table 6.5).

6.6 Summary.

The Amsler machine, and similarly designed machines, have been used world-wide for the assessment of the rolling-sliding wear properties of materials and hence different sets of results have some comparative basis. However, such results are extremely susceptible to the variables within the complete wear test system and the Amsler machine has certain limitations which can affect the reproducibity of such wear test systems. A new wear machine (described in the following chapter) has been developed to overcome such limitations. The results of the wear test programmes on both machines has formed a good comparative basis for assessing the wear behaviour of standard (pearlitic) and experimental (baintic) rail steels. Vibrations, together with the formation of disc surface plastic deformations and the subsequent affect on wear behaviour, were comparatively assessed on both machines.

6.7 References.

Amsler, A.J. (1922). "Abnützungsmaschine für Metalle (Wear machine for metals)." *Z. VDI* 66, pp. 377-378.

Bolton, P.J., Clayton, P. and McEwen, I.J. (1980). "Wear of rail and tyre steels under rolling-sliding conditions." *Proc. ASME/ASLE Lubrication Conf., San Francisco, USA, 18-21/08/80.* Pub. *ASLE Trans.* 25 (1), pp. 17-24.

Bolton, P.J. and Clayton, P. (1984). "Rolling-sliding wear damage in rail and tyre steels." *WEAR* 93, pp. 145-165.

Knothe, K. and Gasch, R., eds., (1983). "Rail corrugations". *Proc. Symp. on "Rail corrugation problems", Inst. für Luft- und Raumfahrt, Tech. Univ. Berlin.*

Ichinose, H., Takehara, J., Iwasaki, N. and Ueda, M. (1978). "An investigation on contact fatigue and wear resistance behaviour in rail steels." *Proc. Ist Int. Conf. on "Heavy Haul Railways", Perth, Australia, September 1978. Inst. Engrs. Austr. and Austr. Inst. Mining and Metallurgy, 1978, Session 307, Paper I3.*

Krause, H. and Lehna, H. (1987). "Investigation of tribological characteristics of rolling-sliding friction systems by means of systematic wear experiments under well defined conditions." *WEAR* 119, pp. 153-174.

Matsumoto, H. Sugino, K. and Hayashida, H. (1978). "Development of wear resistant and anti-shelling high strength rails in Japan." *Proc. Ist Int. Conf. on "Heavy Haul Railways", Perth, Australia, September 1978. Inst. Engrs. Austr. and Austr. Inst. Mining and Metallurgy, 1978, Session 212, Paper H1.*

Vekser, N.A., Kazarnovskii, D.S. and Khurgin, L.S. (1970). "Method for testing wheel and rail steels for wear and contact fatigue galling." Ukranian Scientific Research Inst. of Metals. *Zavodskaya Laboratoriya*, 36 (5), pp. 598-600 (in russian). *Ind. Lab.*, 1970, pp. 760-761 (in english).

Test No.	Top driven disc	Max. contact stress (Mpa)	Initial creep (%)	Test length (x1000 bottom disc revs.)	COMMENT
3	R52	900	3	12	Top disc transverse grainflow
4	R52	900	3	12	Top disc longitudinal grainflow *
5	Repeat of Test 3:		Tests repeated with longer measuring		
6	Repeat of Test 4 :		intervals and amended air cooling.		
7	R52	900	3	50	Air flow increased. Rigid torque arm plus strain gauge fitted.
8	R52	500	3	200	"Mild" wear test.
9	R52	1300	3	20	"Severe" wear test.
10A	R52	1100	3	70:	Reproducibility
10B	R52	1100	3	80:	tests.
10C	R52	1100	3	80	Test speed halved mid-test.
11A	R52	1100	3	70	Test on standard Amsler [@ British Rail]
11B	R52	1100	3	Test faulty	" "
12	R52	1300	ZERO	50	Pure rolling test.
13	R52	474	25	5.9	High creepage test.
13A	B52	833	15	8	High creepage test.
13B	B04	833	15	7	High creepage test.
14	B52	900	3	95	cf. Tests 7 & 16.
15 $	B52 on B52	900	3	100	Bainite on bainite.
16	B04	900	3	90	cf. Tests 7 & 14.
17 $	B04 on B04	900	3	60	Bainite on bainite.
18	B52	500	3	160	cf. Tests 8 & 19.
19	B04	500	3	160	cf. Tests 8 & 18.
20	B52	491	10	60	cf. Tests 21 & 24.
21	B04	491	10	50	cf. Tests 20 & 24.
22	B52	884	10	25	cf. Tests 23 & 25.
23	B04	884	10	10	cf. Tests 22 & 25.
24	R52	491	10	60	cf. Tests 20 & 21.
24A	R52	491	10	50	Repeat test at half speed.
25	R52	884	10	30	cf. Tests 22 & 23.

* Bottom driving disc is W64 except for Tests 15 & 17.
$ All discs were sectioned from rail and wheel tyre to give the grainflow across the wear track except for Tests 4 and 6.

Table 6.1 Amsler wear test programme.

Test No.	Top driven disc	Max. contact stress (Mpa)	Wear surface temperature range over the test period.	
			Top disc	*Bottom disc*
			(°C)	
20	B52	491	29.3 - 31.5	26.0 - 30.2
21	B04	491	31.3 - 32.9	30.4 - 32.0
24	R52	491	31.0 - 34.2	30.0 - 33.6
22	B52	884	32.7 - 34.7	31.9 - 33.8
23	B04	884	35.0 - 37.4	34.3 - 37.0
25	R52	884	35.3 - 38.2	35.0 - 37.3

All tests at 10 % creepage against W64 bottom driving discs.

Temperatures measured by contact probe at each weighing interval immediately the discs had stopped rotating.

Table 6.2 Wear surface temperatures of severe wear test discs.

Test Number		8	19	18	7	16	14	17	15	10B	10C	[c]11A
Top braking disc	:	R52	B04	B52	R52	B04	B52	B04	B52	R52	R52	R52
Bottom driving disc	:	W64	W64	W64	W64	W64	W64	B04	B52	W64	W64	W64
Initial max. contact stress, p_o, (MPa)	:	500	500	500	900	900	900	900	900	1100	1100	1100
Initial creepage, γ, (%)	:	3	3	3	3	3	3	3	3	3	3	3
Nominal p_o? (MPa)	:	15	15	15	27	27	27	27	27	33	33	33
Test speed (top disc Hz)	:	5.83	5.83	5.83	5.83	5.83	5.83	5.83	5.83	5.83	5.83	5.83
Profiled at (bottom disc cycles X 10^3)	:	200	160	160	50	90	95	60	100	70	60-	80	70
(ie, at the test end unless indicated*)												
Track width spread (%)	Top	:	2.0	2.0	0.8	9.4	14.3	2.4	13.2	2.6	24.3	-	21.9	19.3
	Bottom	:	1.5	2.4	2.2	9.6	23.7	6.2	14.5	4.0	24.4	-	22.8	25.0
Disc eccentricity (μm)	Top	:	5		2	np	np	np	6	14	22	25	33	40
	Bottom	:	7	3	10	np	np	np	6	12	60	60	67	25
Max. amplitude of long wave-]_	Top	:	-	-	-	np	np	np	45F	-	4.5ip	71	9.51	18F
length undulations [($\pm\mu$m) [a]]	Bottom	:	-	-	-	np	np	np	14F	-	201	181	151	121
Facets per circumference	Top	:	-	-	-	np	np	np	21	-	-	-	-	122
	Bottom	:	-	-	-	np	np	np	29	-	-	-	-	-
Facet frequency	Top	:	-	-	-	np	np	np	122	-	-	-	-	-
	Bottom	:	-	-	-	np	np	np	187	-	-	-	-	-
Max. amplitude of short wave-]_	Top	:	1	0.5	2	np	np	np	2	8	3.5	5	1C	6C
length undulations ($\pm\mu$m) [b]]	Bottom	:	6	6	2	np	np	np	2	5	8	14	2C	3C
Corrugations per circumference	Top	:	-	-	-	2547	2307	2384	-	-	-	-	1249	2349
	Bottom	:	-	-	-	2625	2402	2456	-	-	-	-	1218	2468
Corrugations per cm of]_	Top	:	-	-	-	33	31	31	-	-	-	-	33	31
circumference]	Bottom	:	-	-	-	33	31	31	-	-	-	-	31	31

Test Number		9	24	24A	21	20	25	23	22	13	13B	13A
Top braking disc	:	R52	R52	R52	B04	B52	R52	B04	B52	R52	B04	B52
Bottom driving disc	:	W64	W64	W64	W64	W64	W64	W64	W64	W64	W64	W64
Initial max. contact stress, p_o, (MPa)	:	1300	491	500	491	491	884	884	884	474	833	833
Initial creepage, γ, (%)	:	3	10	10	10	10	10	10	10	25	15	15
Nominal p_o? (MPa)	:	39	49	50	49	49	88	88	88	119	125	125
Test speed (top disc Hz)	:	5.83	5.83	2.92	5.83	5.83	5.83	5.83	5.83	5.83	2.92	2.92
Profiled at (bottom disc cycles X 10^3)	:	20	60	50	50	60	30	10	25	5.9	7	8
(ie, at the test end unless indicated*)												
Track width spread (%)	Top	:	25.1	5.7	7.6	20.5	2.4	25.2	21.0	5.2	25.5	22.0	4.9
	Bottom	:	23.3	6.4	6.4	15.9	11.3	16.8	31.6	33.0	10.9	37.5	23.5
Disc eccentricity (μm)	Top	:	20	20	5	2	10	27	12	5	50	7	30
	Bottom	:	65	10	10	10	18	25	45	30	90	29	38
Max. amplitude of long wave-]_	Top	:	-	8F	-	-	40F	20F	45R	10R	95F	40R	-
length undulations ($\pm\mu$m) [a]]	Bottom	:	201	12F	13F	52F	62F	40F	85F	50F	-	105F	-
Facets (or Ripples)]_	Top	:	-	10	-	-	4	21	85	53	8	32	-
per circumference]	Bottom	:	-	10	20	3	9	11	12	12	-	3	-
Facet (or Ripple) frequency	Top	:	-	58.3	-	-	23.3	122.4	496	309	46.6	93.3	-
	Bottom	:	-	64.3	64.3	19.3	57.9	70.7	77.2	77.2	-	9.6	-
Max. amplitude of short wave-]_	Top	:	8		6C	3C	2	2	25	10	18	45	12
length undulations ($\pm\mu$m) [b]]	Bottom	:	15	4C	0.5C	18	2	2	27	9	30	32	20
Corrugations per circumference	Top	:	-	2258	1193	-	2047	-	-	-	-	-	-
	Bottom	:	-	2335	1238	-	-	-	-	-	-	-	-
Corrugations per cm of]_	Top	:	-	30	31.5	-	27	-	-	-	-	-	-
circumference]	Bottom	:	-	28	29.5	-	-	-	-	-	-	-	-

[a] : "np" - disc not profiled (visual count of corrugations).
"y" - long wavelength corrugations formed, termed "facets".
"R" - long wavelength ripples formed; these are not track wide.
"i" - irregular facet wavelengths.
"p" - only partial facet formation around the disc circumference.

[b] : A measure of irregular surface roughness or, "C", the amplitude of regular short wavelength corrugations.

[c] : Test carried out (with smaller test discs) on a conventional Amsler machine at British Rail Research, Derby, UK.

Table 6.3 Test disc deformations, including periodic undulations, generated during the test programme. Test conditions are shown.

Maximum contact stress (MPa)	Creepage 0%	3%	6%	10%	25%
R52 / W64					
474					
491					(F/none)
500		(none/none)		(C,F/C,F)	
629			(C,F/C,F)	(C,F/C,F)	
850		(C/C)			
884				(F/F)	
900		$(C/C)^{np}$			
1000		(none/none)			
1100		(none/none)			
1100*		$[(C,F/C)]^{*@\ Derby}$			
1300	$(none/none)^{np}$				
B04 / W64					
491					
500		(none/none)		(none/F)	
884					
900		$(C/C)^{np}$		(none/F)	
900*		$(F/F)^{*B04\ both\ discs}$			
B52 / W64					
491					
500		(none/none)		(C,F/F)	
884					
900		$(C/C)^{np}$		(none/F)	
900*		$(none/none)^{*B52\ both\ discs}$			

KEY:

C	: corrugations formed.
F	: facets formed.
(F,C/F)	: top disc, facets and corrugations / bottom disc, facets only.
none	: no regular undulations formed.
np	: discs not profiled for facet detection.
@ Derby	: comparative test on conventional Amsler at British Rail Research, Derby.

Table 6.4 Test condition map for form of Amsler disc surface undulations.

Static disc contact results

(* this reading may be influenced by low frequency probe noise)
Many possible harmonics exist within all the results shown. For the sake of clarity they are not indicated.

Transducer Location	Principal Frequencies (Hz)		Signal Strength (mV)
STEEL Hammer			
Top bearing housing			
Accelerations:	4950	peak	32
	(4500-5700)	range	>10
	1550		20
	1025		11
	500, 675		≈ 6
Velocities:	500		2.8
	1550		2.3
	75		2.0
	4950		1.5
	675, 1025, 1325		≈ 0.8
Bottom bearing housing			
Accelerations:	5000	peak	38
	(4500-5500)	range	>10
	1575		10
	1050		5
	500, 675, 850		≈ 3
Velocities:	1550		3.3
	500		3.0
	1025		2.1
	*25, 675		1.3

Transducer Location	Principal Frequencies (Hz)	Signal Strength (mV)
SOFT Hammer		
Top bearing housing		
Accelerations:	500	90
	1025	48
	675	40
	775	30
	1525	20
	4600	9
Velocities:	475	8.0
	* 25	6.3
	100	5.3
	225, 675	2.7
	1025	1.8
Bottom bearing housing		
Accelerations:	500	58
	1025	48
	675	33
	800	27
	950	22
	1500	18
	4600	6
Velocities:	500	7.8
	* 25	5.1
	675	3.1
	750, 1025	1.8
	1550	0.4

Table 6.5 Principal natural resonances, measured as accelerations and velocities, of the modified Amsler in static mode with excitations from hard (steel) and soft (polymer) hammer blows.

NO DISCS, MACHINE FREE RUNNING

The top bearing housing was pivoted down against a 10mm rubber stop and loaded to 36 kgf (equivalent to 500 MPa p_o if discs were present). It believed JRB carried out this test with the bearing pivoted up in the raised (rest) position with no load applied, although JEG is not positive about this. The machine was tested at both motor speeds, equivalent to 386 and 193 bottom disc rpm. The shaft speeds and gear impact frequencies are shown in Figure 2.

Transducer Location	Principal Frequencies (Hz)	Signal Strength (mV)
386 rpm		
Top bearing housing		
Accelerations:	425	180
	837.5	35
	1262.5	30
	212.5, 687.5, 1137.5	15 → 22
	962.5, 2450	11 → 14
	50	4
Velocities:	420	15.6
	20, 50, 210, 840	2.0 → 2.8
Bottom bearing housing		
Accelerations:	425	244
	837.5	39
	625	32
	550, 1050, 1262.5	14 → 19
Velocities:	420	25.6
	*5, 20, 240, 300, 540, 625, 840	1.4 → 2.3

Transducer location	Principal Frequencies (Hz)	Signal Strength (mV)
193 rpm		
Top bearing housing		
Accelerations:	425	44
	212.5	25
	650, 800, 1262.5	6 → 9
	62.5, 2475	±3
Velocities:	212.5	6.3
	425	5.5
	62.5	1.7
	625, 800, 1262.5	±0.7
Bottom bearing housing		
Accelerations:	425	37
	625	35
	875	14
	212.5	10
	2912.5	8
	150	5
Velocities:	425	4.3
	625	2.8
	212.5	2.2
	*12.5, 150, 325	±1.5
	875	0.7
	2912.5	0.2

Table 6.6 Principal resonances, measured as accelerations and velocities, of the modified Amsler free running with no discs.

MACHINE UNDER LOAD AT BOTH SPEEDS

Corrugated and faceted discs from Test JB5 (386rpm) and Test 24A (193rpm) were fitted so that they were nominally loaded to give 500 MPa maximum contact stress with 10% creepage. Both sets of tests discs had already run for 50,000 (bottom disc) revolutions. Vibration checks were made over an extra few thousand revolutions using these worn discs.

Transducer Location		Principal Frequencies (Hz)		Signal Strength (mV)
386rpm.	Test JB5	Corrugations	Facets	
	Top disc:	2121	58.2	
	Bot.disc:	2178	64.3	
Top bearing housing				
Accelerations:		62.5		324
		425		270
		125, 250, 825, 1625, 2475, 4750, 5350		40 → 70
Velocities:		65		146
		417.5		26
		45, 127.5, 440		10 → 15
Bottom bearing housing				
Accelerations:		425		116
		62.5		53
		600		35
		837.5		28
		1250, 4625 → 5000		20
		2975, 4175		≈10
Velocities:		57.5 → 65		25
		420		11
		22.5, 122.5, 180, 302.5, 360, 442.5, 470		1 → 5

Transducer Location		Principal Frequencies (Hz)		Signal Strength (mV)
193 rpm	Test 24A	Corrugations	Facets	
	Top disc	1193	-	
	Bot.disc	1238	64.3	
Top bearing housing				
Accelerations:		62.5 → 65		183
		125 → 130		55
		210 → 212.5, 425		40
		662.5		19
		1112.5		12
		2300, 4850		7
Velocities:		65		104
		130		19
		210		8
		420		3
Bottom bearing housing				
Accelerations:		62.5 → 65		35
		625		34
		375		28
		725 → 785		17
		125, 200, 962.5, 4225, 4600, 5000, 5525		9 → 12
Velocities:		65		18
		127.5, 192.5, 375, 630		2 → 4

Table 6.7 Principal resonances, measured as accelerations and velocities, of the modified Amsler running with worn discs at two test speeds, set at 500 MPa maximum contact stress and 10% creepage. Test JB5 was part of the initial analysis[Garnham et al, 1988. Appended reference - Appendix I] with above test conditions, at the higher speed, with spring loading.

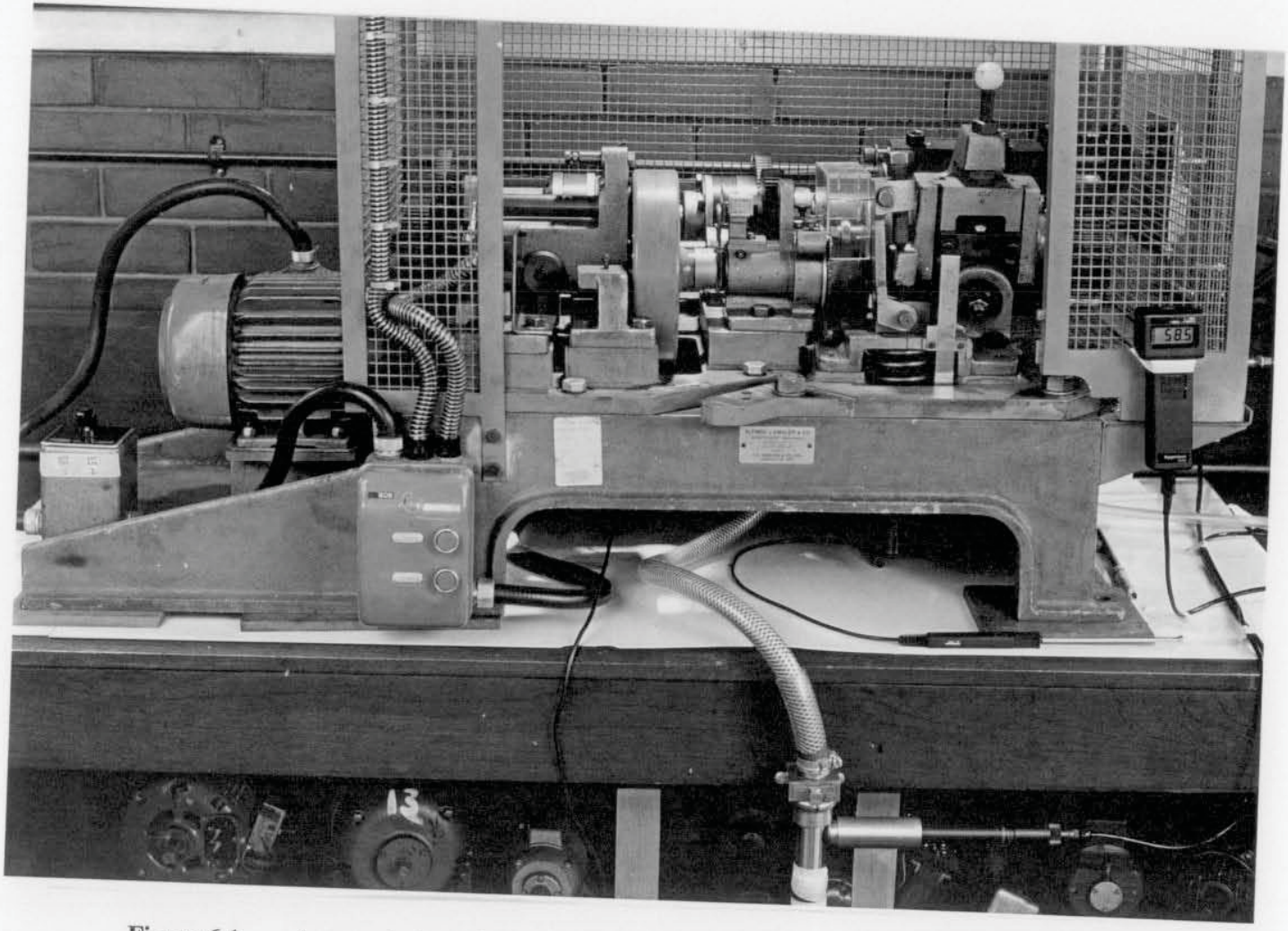

Figure 6.1 A general view of the modified Amsler wear machine. The test discs can be seen beneath the perspex cover of the environment chamber. The debris filter unit and the humidity probe are at the front of the bench.

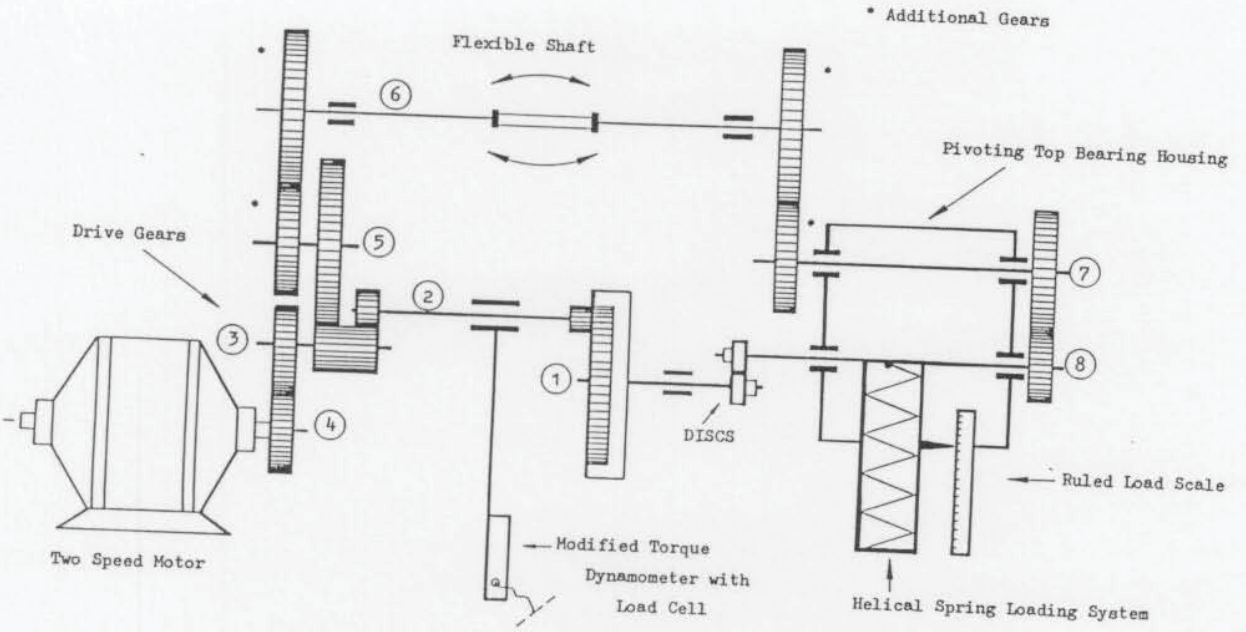

AMSLER SHAFT AND GEAR TOOTH CONTACT FREQUENCIES

Amsler set at "400" rpm

SHAFT NUMBER	SHAFT rpm	SHAFT Hz	NUMBER OF GEAR TEETH	TOOTH CONTACT FREQUENCIES (Hz)	DESCRIPTION
1	386	6.43	100	643	Bottom shaft and disc
2	1287	21.4	30 35	643 751	Dynamometer
3	1287	21.4	35 72	751 1544	Linking gear for top and bottom shafts
4	2988	49.8	31	1544	Motor drive
5	450	7.51	100 56	751 420	*
6	308	5.13	82	420	* Additional yaw gears
7	450	7.51	56 59	420 443	*
8	350	5.83	76	443	Top shaft and disc

Amsler set at "200" rpm

1	193	3.22	100	322	Bottom shaft and disc
2	643	10.7	30 35	322 375	Dynamometer
3	643	10.7	35 72	375 772	Linking gear for top and bottom shafts
4	1494	24.9	31	772	Motor drive
5	225	3.75	100 56	375 210	*
6	154	2.57	82	210	* Additional yaw gears
7	225	3.75	56 59	210 221	*
8	175	2.92	76	221	Top shaft and disc

Figure 6.2 A schematic view of the modified Amsler machine used for this work, together with shaft speeds and gear tooth contact frequencies.

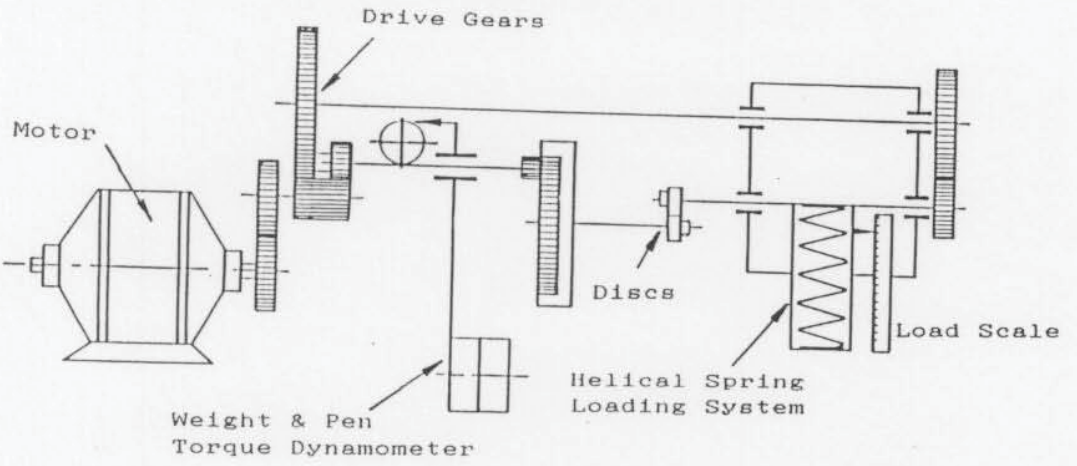

Figure 6.3 A schematic view of a conventional Amsler machine, as used for most British Rail Research tests.

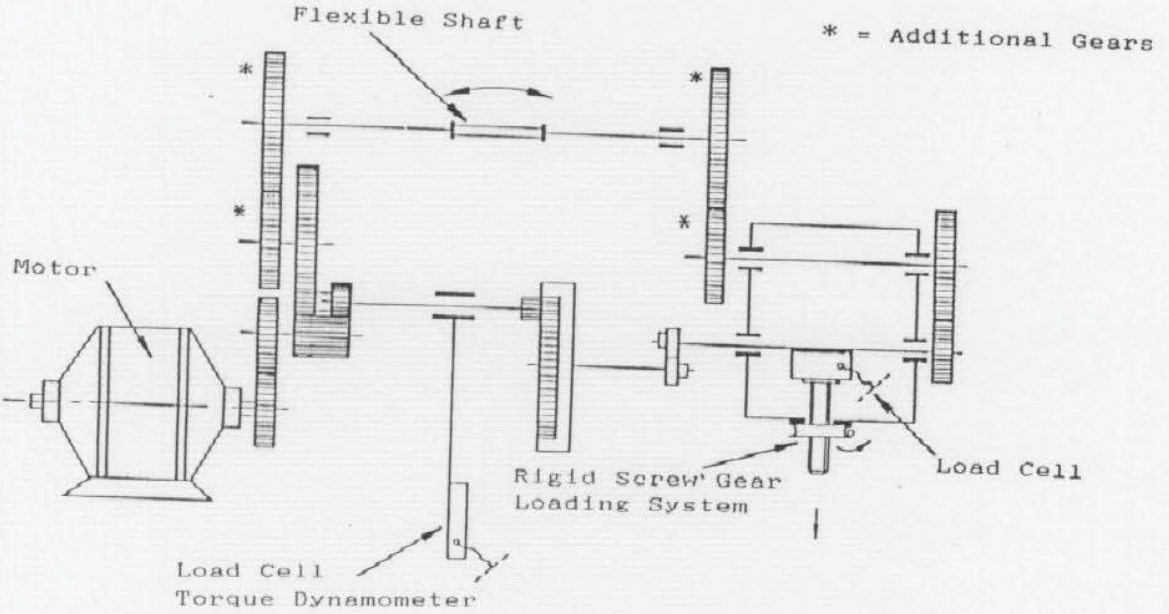

Figure 6.4 A schematic view of the modified Amsler machine, with spring loading replaced by rigid loading, as used for part of the initial vibration analysis[Garnham et al, 1988; appended - Appendix I]

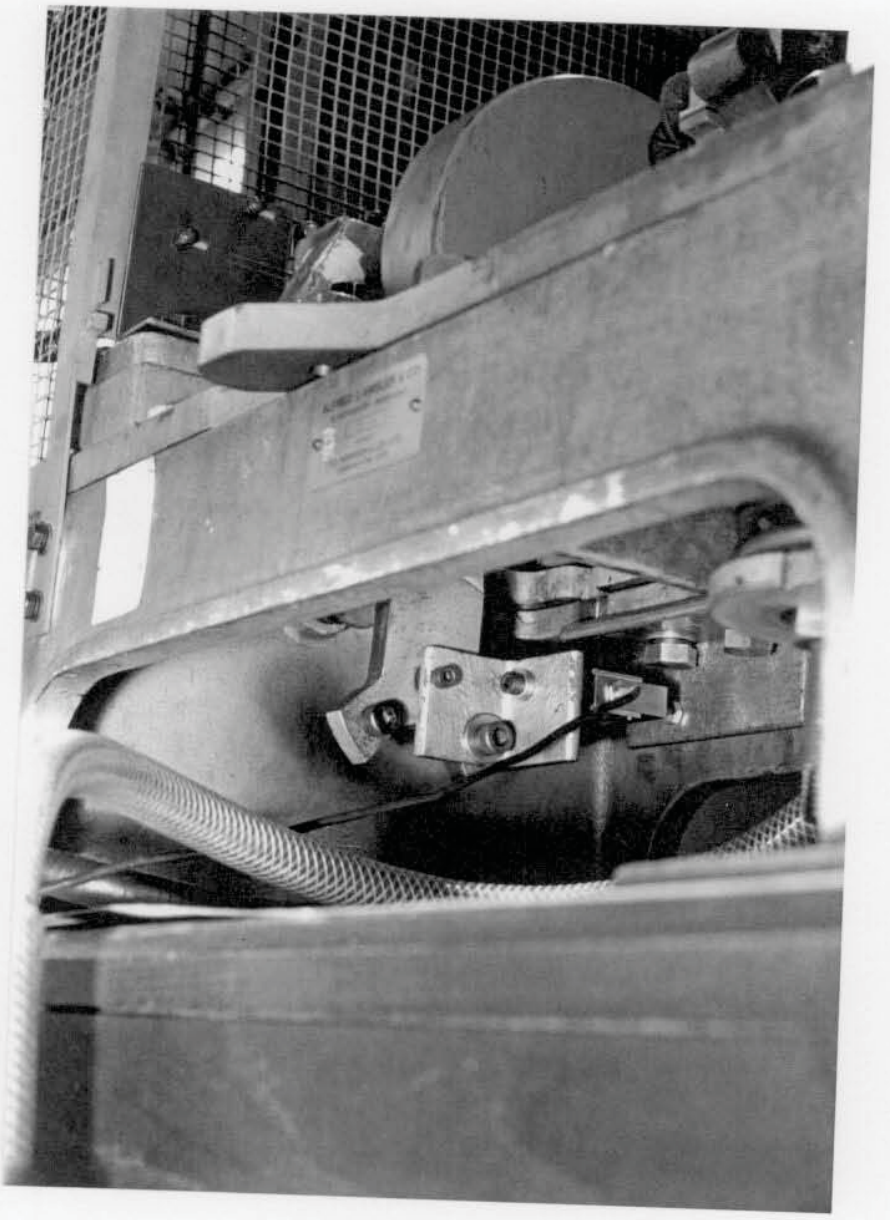

Figure 6.5 The location of the rigid torque measuring arm and load cell added to the modified Amsler.

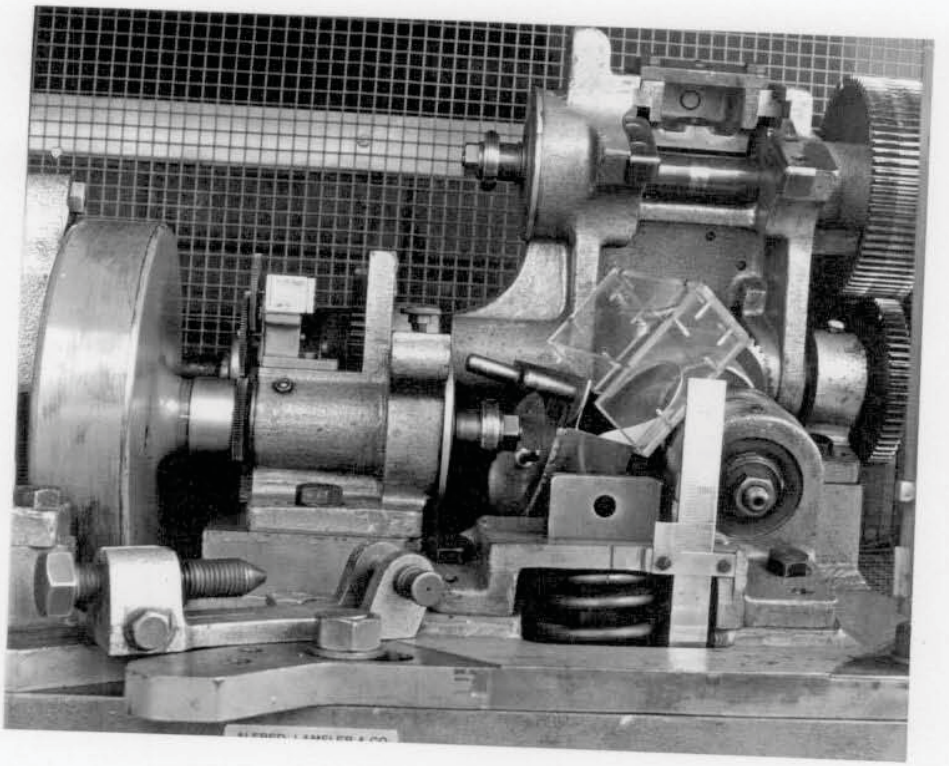

Figure 6.6 The modified Amsler set for disc loading.

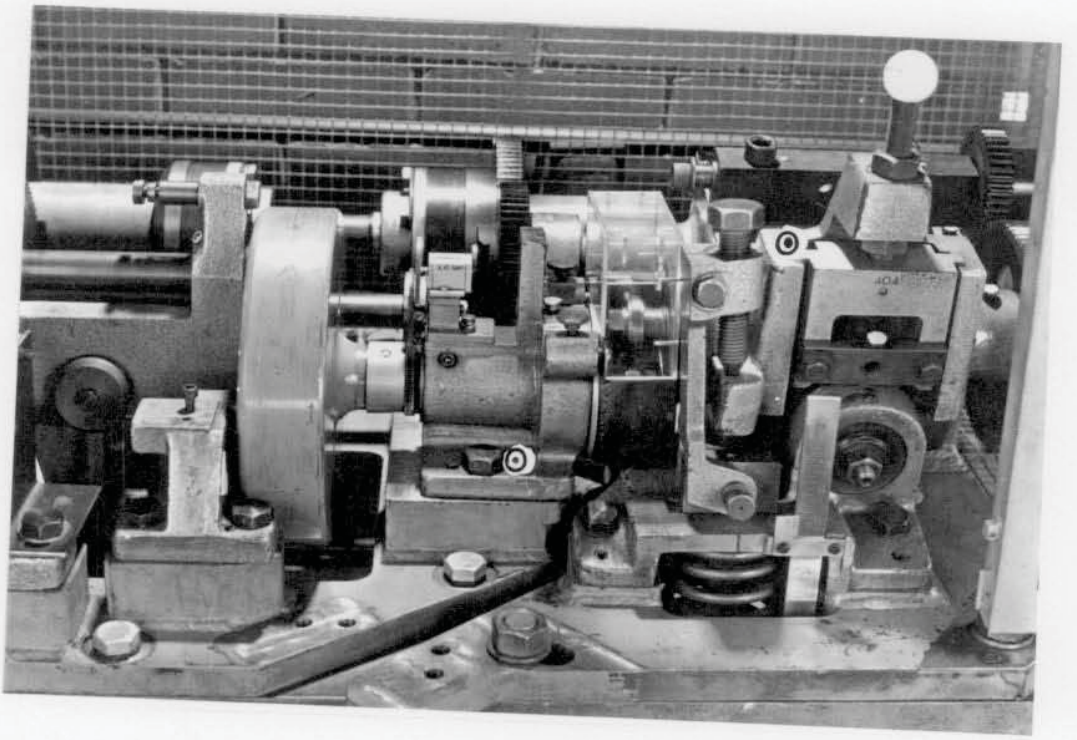

Figure 6.7 The modified Amsler during a test run. The locations of the accelerometers used for the later vibration analysis are shown thus ◎. For the initial analysis[Appendix I], the top location was on the curved surface of bearing housing, hidden by the bolt. The amended position shown was steadier.

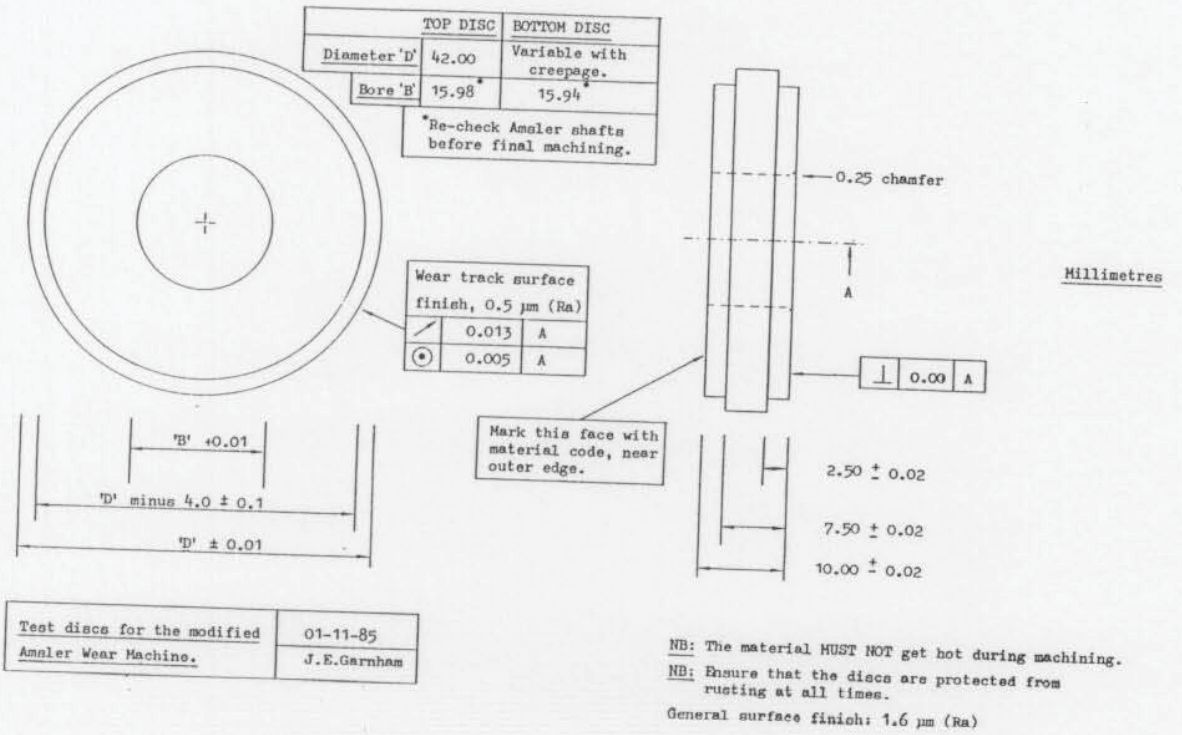

Figure 6.8 Amsler disc dimensional specification.

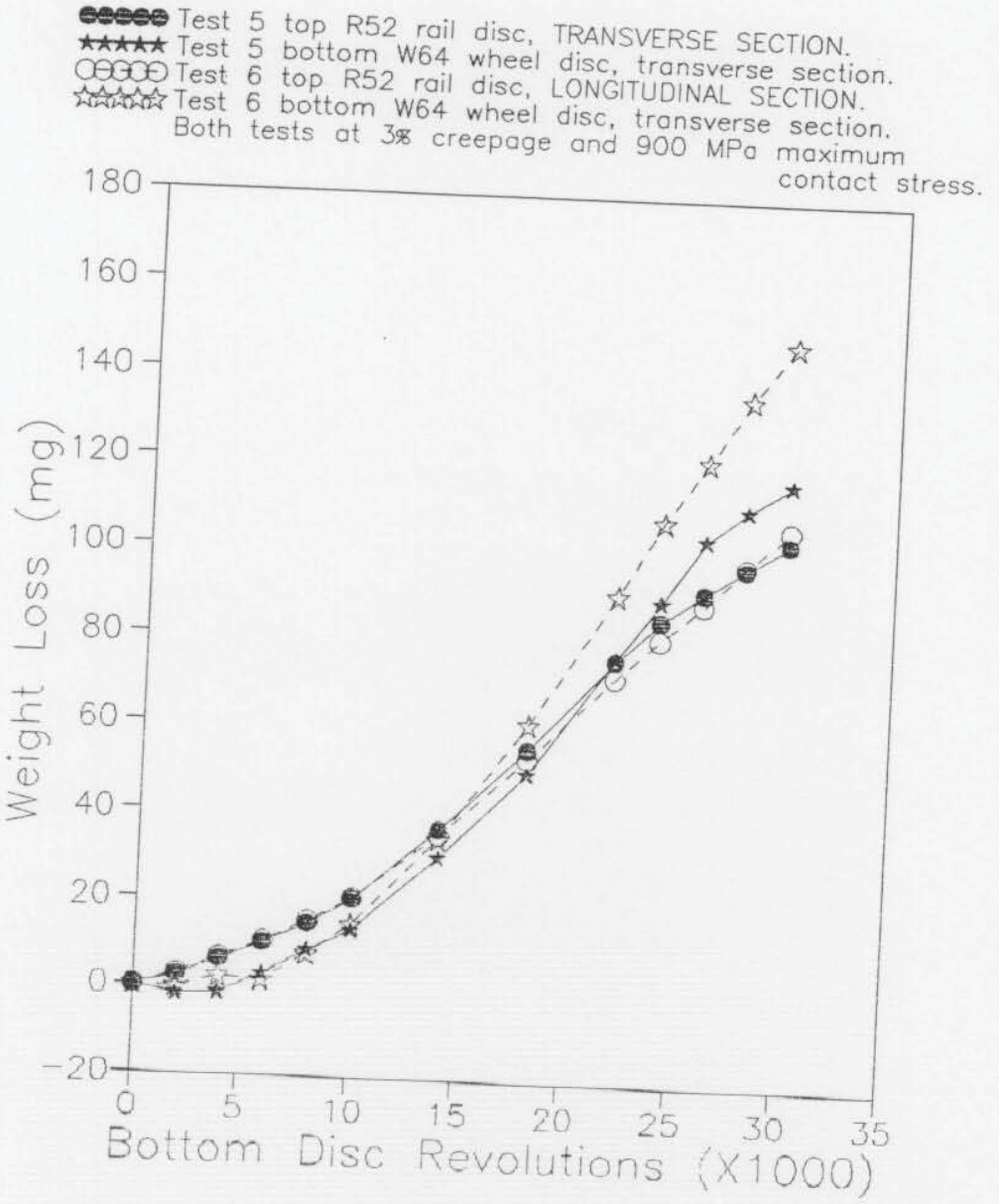

Figure 6.9 The effect of changing the top disc grainflow direction on wear curves.

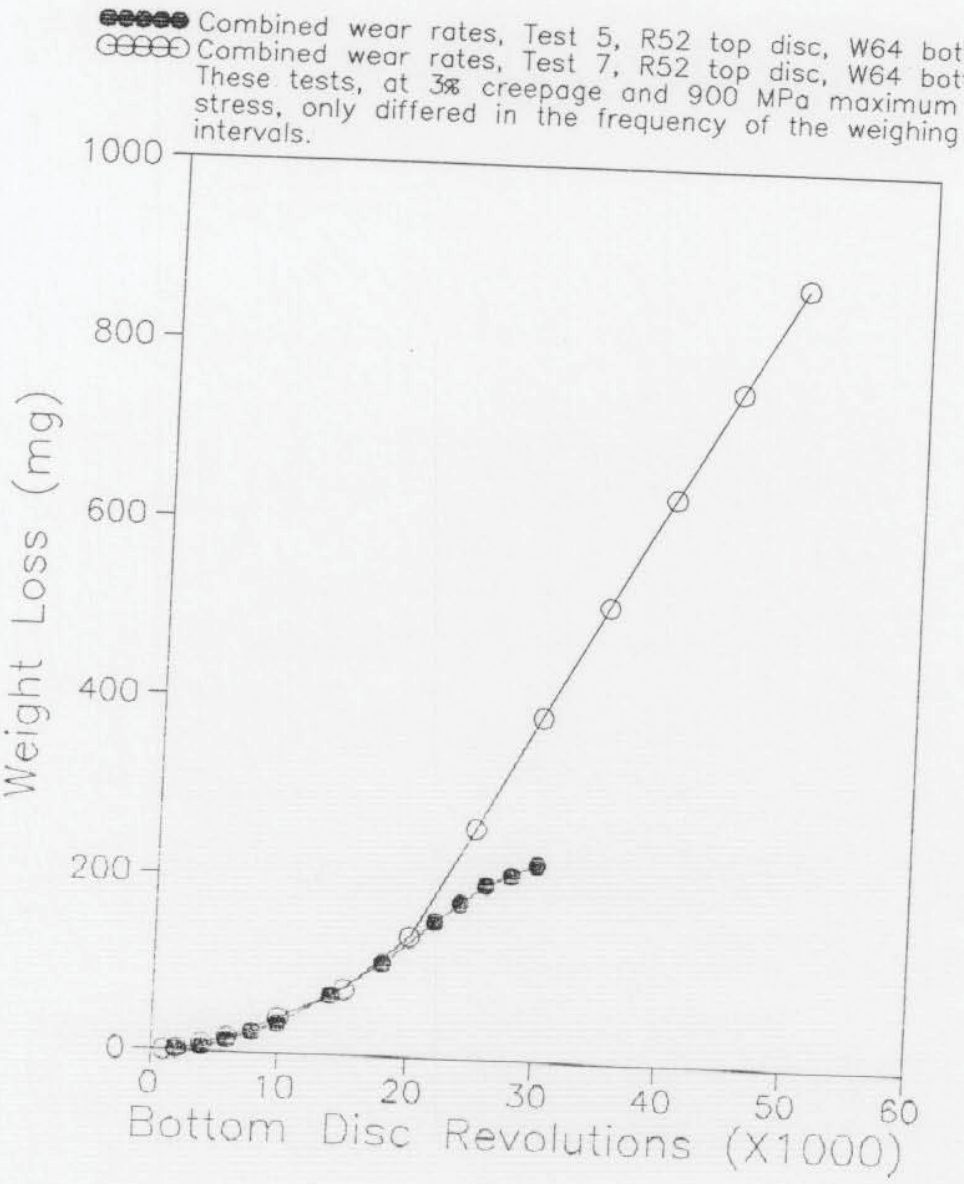

Figure 6.10 The effect of changing weighing intervals on combined top and bottom disc wear rate.

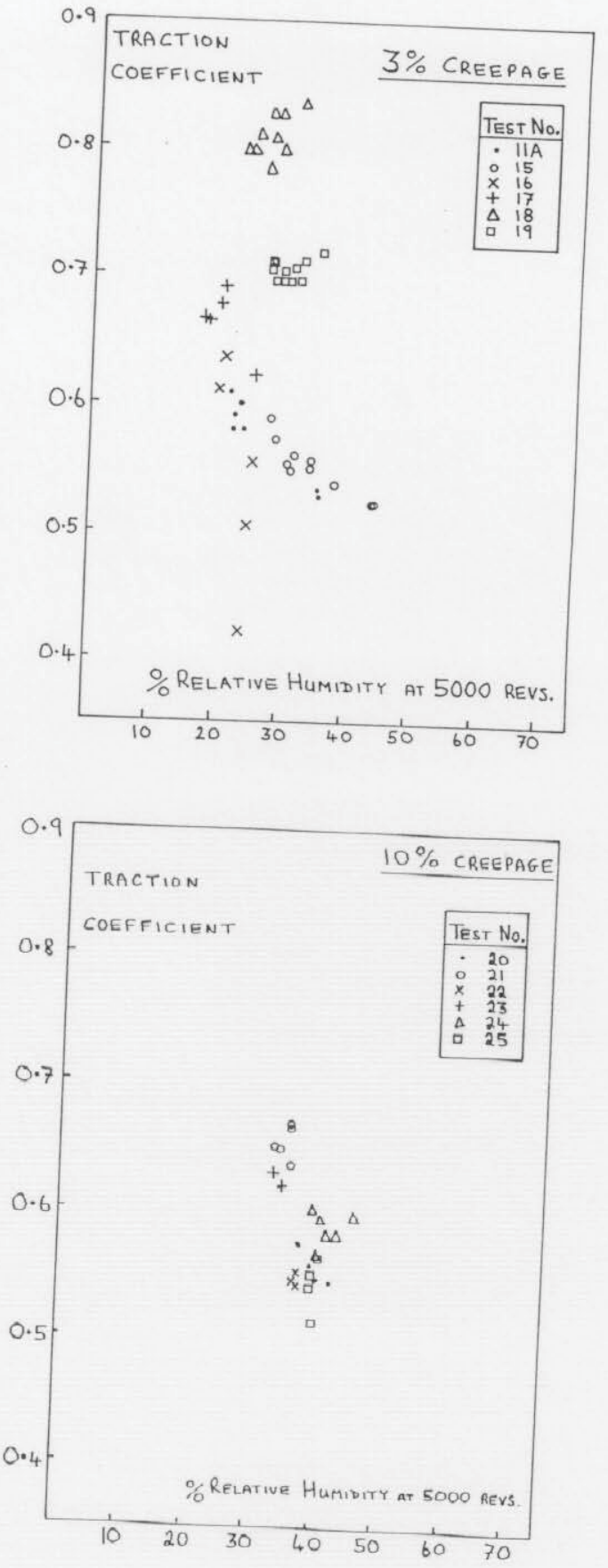

Figure 6.11 The variation of traction coefficient with changes in environment chamber humidity for tests at two creepage levels.

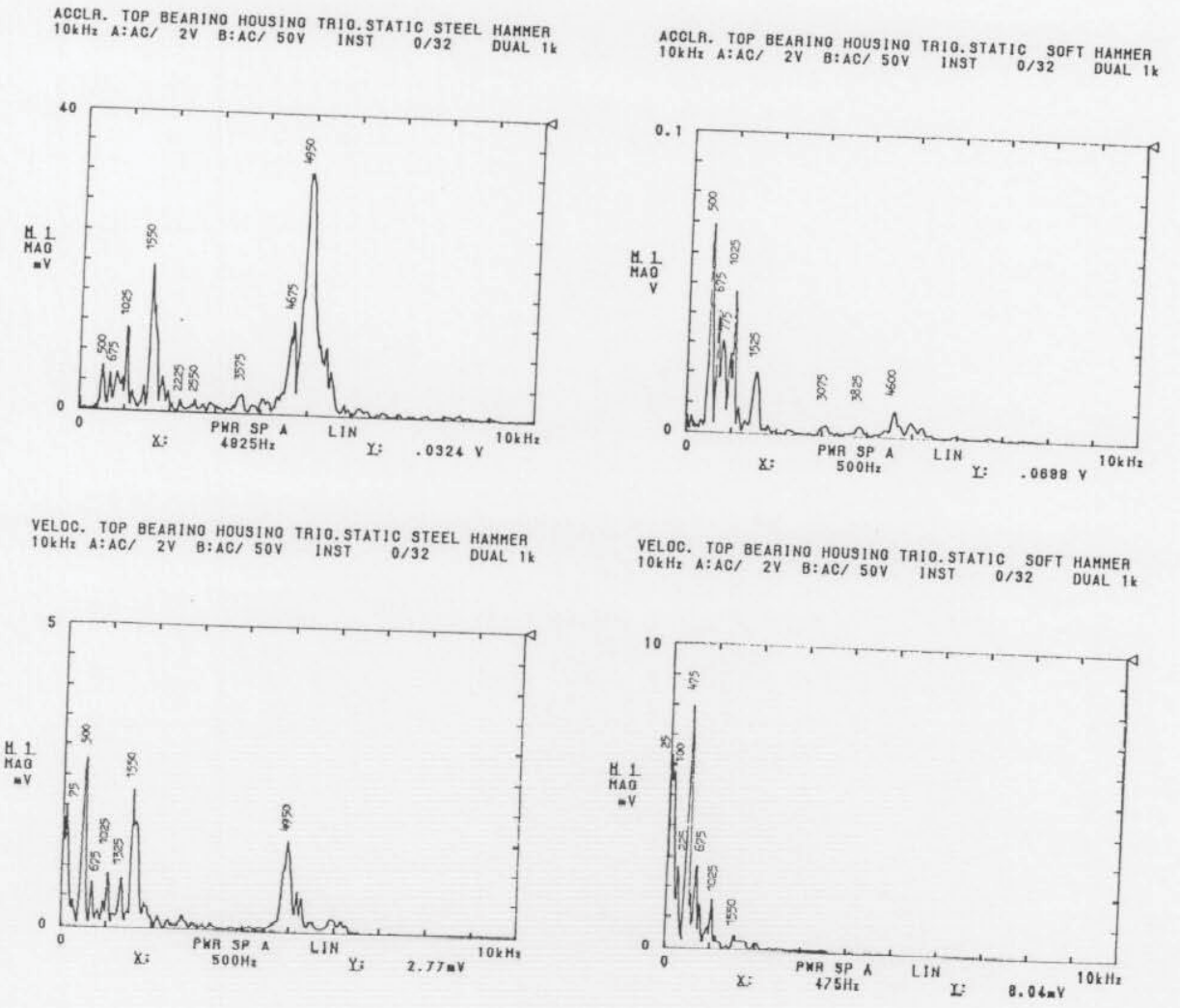

Figure 6.12 Modified Amsler vibration frequency spectra. Natural resonances, measured as accelerations (top figures) and velocities (bottom figures), of the top bearing housing for a static machine excited by hard steel hammer blows (leftside figures) and soft polymer hammer blows (rightside figures).

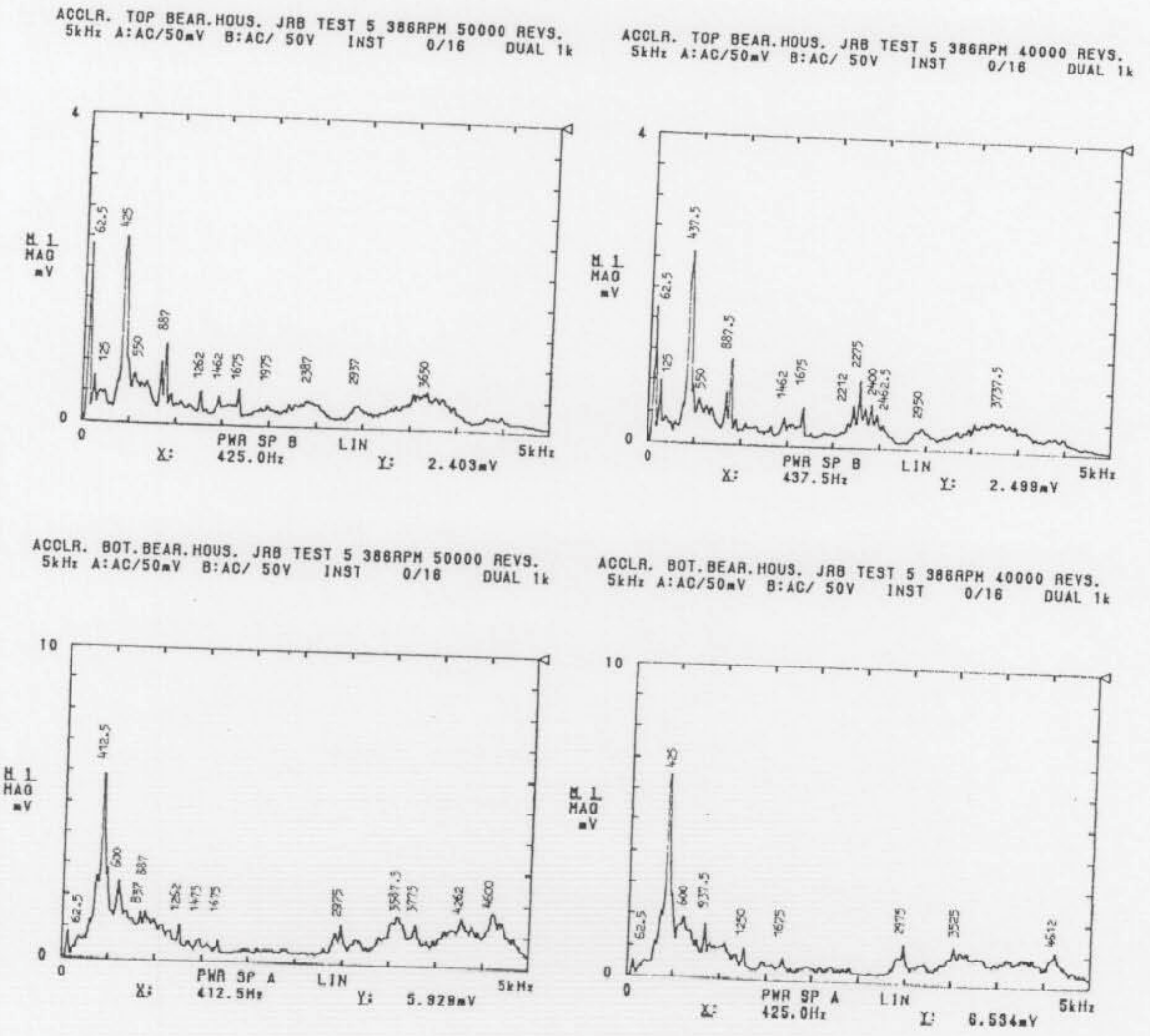

Figure 6.13 Modified Amsler vibration frequency spectra, measured during the initial analysis[Appendix I], of a discs tested at 500 MPa maximum contact stress amd 10% creepage, with spring loading. Resonances, measured as accelerations, of the top and bottom bearing housings (top and bottom figures, respectively) are shown, at 50000 and 40000 bottom disc revolutions (leftside and rightside figures, respectively).

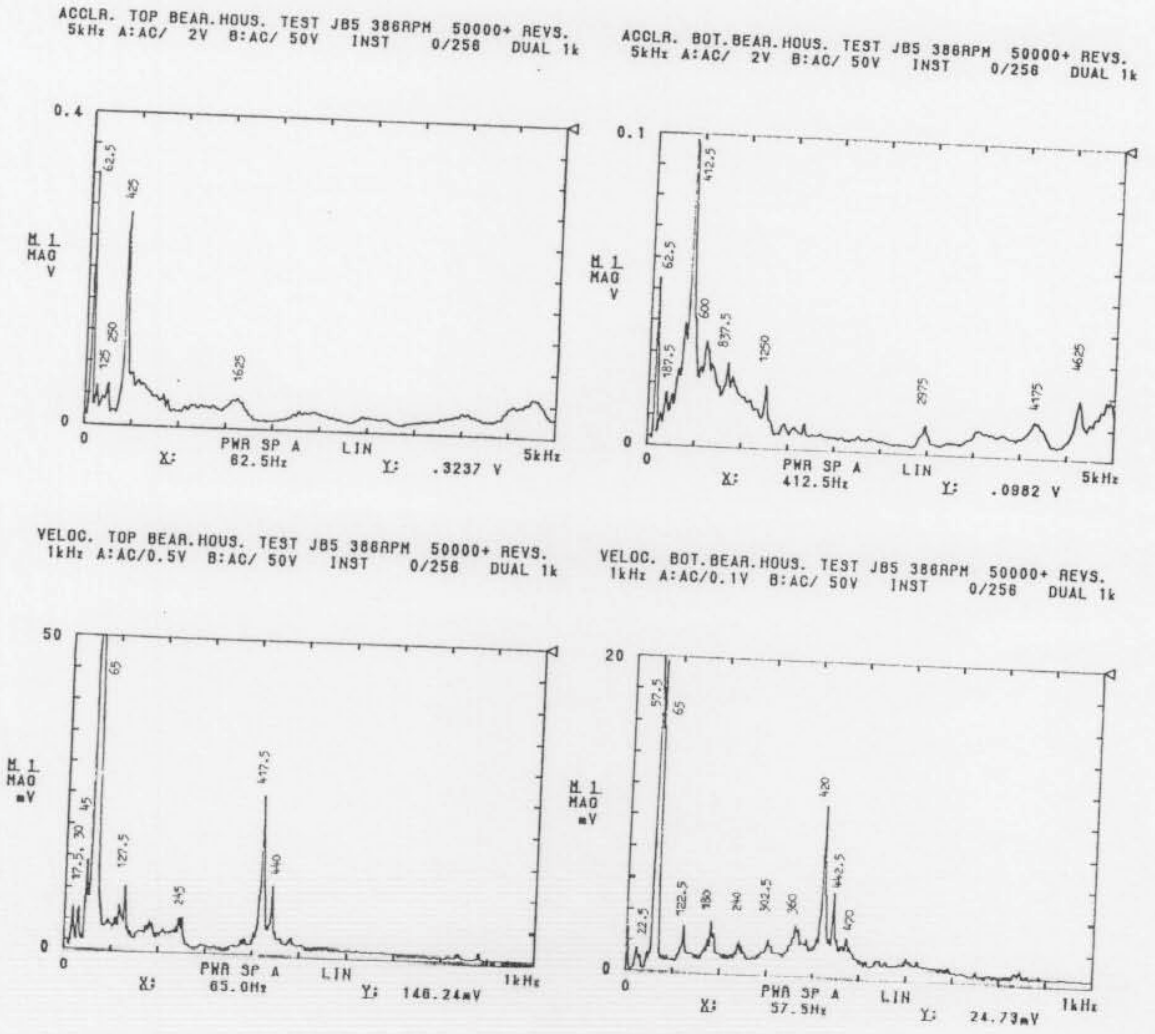

Figure 6.14 Modified Amsler vibration frequency spectra measured during a repeat analysis. A re-assessment of resonances generated by using the worn, 50000 + revolution tests discs whose resonances are shown in Figure 6.13. Accelerations and velocities were measured (top and bottom figures, respectively) on the top and bottom bearing housings (leftside and rightside figures, respectively).